JETIR.ORG ISSN: 2349-5162 | ESTD Year : 2014 | Monthly Issue
JOURNAL OF EMERGING TECHNOLOGIES AND INNOVATIVE RESEARCH (JETIR)
An International Scholarly Open Access, Peer-reviewed, Refereed Journal

Synthesis, Crystal growth, structure and characterization of mixed crystals of zinc potassium hydrogen phthalate $[C_{16}H_{17}KO_{13}]_2Zn$ - centrosymmetric crystal exhibiting SHG activity

Shaik Alla Nazeer[1] , G. Ramasamy[1,2] *
[1]*Department of Chemistry, Annamalai University, Annamalai Nagar 608002, India*
[2]*Department of Chemistry, Government Thirumagal Mills College, Gudiyattam, Vellore Dt. Tamilnadu 632602*

ABSTRACT

Single crystals of zinc(II) incorporated potassium hydrogen phthalate $[C_{16}H_{17}KO_{13}]_2Zn$ (ZKP) were grown from an aqueous solution containing potassium hydrogen phthalate and zinc sulphate in the molar ratio (6:1) by using slow evaporation solution growth method at room temperature. The ZKP mixed crystal belongs to the monoclinic system with the space group $P2_1/c$ and the cell parameters are, a = 10.4151(4) Å , b = 6.849 (3) Å , c = 29.4743(12) Å , $\alpha = \gamma = 90°$ and $\beta = 98°(1)$. The grown mixed crystals were further characterized using FT-IR, SEM, EDS, UV-vis spectra and SHG measurements. The hydrogen bonding contribution percentage is analyzed using Hirshfeld surfaces fingerprint plots. The mechanical strength of mixed crystal ZKP was investigated using Vickers microhardness technique. Intrustingly we observe that a centrosymmetric structured mixed crystal ZKP exhibiting second harmonic generation (SHG) activity, contrary to expectations and the results are rationalized. Z-scan procedure determine for third-order nonlinear optical properties by the help of He-Ne laser. Closed aperture Z-scan study gives the positive nonlinearity in ZKP and open aperture Z-scan illustrate the nonlinear absorption is reverse saturation absorption.

Keywords: Crystal growth, Crystal structure, Characterization methods, Mixed crystal.

1. Introduction

Phthalic acid derivative crystals are potential candidates for nonlinear optic properties. Acid phthalate crystal is crystallized eaither centrosymmetric or noncentrosymmetric structures depending on the nature of metal ions, in three dimensional crystallographic array frame work, the bonding orientation is dramatically determined by the cations, on the basis of theories of chemical bonding of single crystal growth **[1,2]**. Potasssium hydrogen phthalate (KHP) is well known for its application in non linear optical properties and the preparation of crystal analyzer for long-wave X-ray spectrometer applications **[3,4]** . It possesses pyroelectric, piezoelectric and nonlinear optical properties **[5-8]**. It crystallizes in orthorhombic system with the space group $Pca2_1$ **[9]**.

In some of the cases the crystals with centrosymmetric space group exhibiting considerable SHG efficiency is reported, guanidinium trifluoroacetate crystral [**10]**, glycine picrate **[11]**, effect of Fe^{3+}-doped bis(thiourea)zinc chloride crystals **[12]**, NLO activity of tthiourea nickel(II)nitrate crystals **[13]**, dibenzoylcroconate **[14]** and the mixed crystal $K_{0.78}Na_{1.22}[C_6H_4(COO)_2]\ H_2O$ **[15]**.

In this work, we report the growth, structure and characterization of the new mixed crystal, zinc incorporated KHP [ZKP] belonging to centrosymmetric system exhibiting SHG - acitvity and the results are rationalized.

2. Experimental

2.1. Synthesis and Crystal growth

The mixed crystal ZKP was grown from an aqueous solution containing potassium hydrogen phthalate (KHP) and zinc sulphate in the molecular ratio of 6:1, using triply distilled water as solvent, stirred well for 3 h using magnetic stirrer to ensure homogeneity. The solution was tightly covered using perforated paper. Transparent good quality crystals were grown from the aquous growth medium after a 20 days. Photographs of the mixed crystal ZKP is shown in **Fig.1.**

2.2. Characterization techniques

In order to determine the crystal structure, purity and identification, single crystal X-ray diffraction data were collected with a specimen 0.45 x 0.30 x 0.30 mm^3 cut out from the grown crystals using an Oxford Diffraction Xcalibur-S CCD system equipped with graphite monochromated Mo$K\alpha$(λ=0.71073 Å) radiation at 293 K. The

structure of mixed crystal was solved by the methods (SHELXS-97) and refined by full-matrix least squares against F^2 using SHELXL-97 software **[16]**.The molecular structure of mixed crystal was drawn using ORTEP-3. The powder XRD analysis was done by using Philips Xpert Pro Triple-axis X-ray diffractometer. The XRD data are analyzed by Rietveld method with RIETAN-2000. The FT-IR spectrum of ZKP crystal was recorded in the of range 4000-400 cm^{-1} using AVATAR 330 FT-IR using KBr pellet technique. The UV-vis analysis was carried out in the region 200 to 800 nm using the Perkin Elmer Lambda 35 model spectrophotometer. Kurtz powder SHG method used for the second harmonic generation test **[17]**.

2.3. Computational details

The Hartree–Fock [HF] calculation was performed using *GAUSSIAN09W* **[18]** program package on a computer without any constraint on the geometry using LANL2DZ basis set **[19]**. Optimized structure of the molecule has been visualized using the GAUSSVIEW molecular visualization program **[20]**. The Surface analysis was done using HF method with 3-21G as basis set, using single crystal XRD data.

3. Result and Discussion

3.1. FT-IR

The FT-IR spectrum of ZKP mixed crystal is shown in **Fig.2.** Comparison of the characteristic vibrational patterns of ZKP with that of the parent compound reveals shifts in some of the characteristic vibrational frequencies. It could be due to the lattice stress developed by the incorporation of Zn(II) into the crystalline matrix. The O-C=O and C=O and stretching frequencies appear at 1475 and 1691 cm^{-1} respectively. The characteristic vibrational patterns of the mixed crystal ZKP and KHP are given in the **Table 1.**

3.2. SEM analysis

The SEM pictures of ZKP crystals at three different magnifications are given in **Fig.3.** It exposes the surface roughness is due to the structure defect centres and voids.

3.3.UV-visible

The UV-visible spectrum of the mixed crystal ZKP gives high reflectance in the visible region and the lower cut-off wave length is found at ~293 nm. Incorporation of foreign metal zinc(II) ion into the KHP crystal lattice not destroy the optical transmission of KHP.

The strenth of an absorbing species can be determined using the Kubelka-Munk equation **[21]** correlating reflectance and concentration, The direct band gap energy obtained from the intercept of the straight lines of Tauc plot with energy axis at $[F(R)\ h\upsilon]^2 = 0$ (**Fig. 4**) are deduced as 3.8 eV.

3.4. X-ray diffraction analysis

The powder XRD pattern of ZKP crystal reveals that the sample is of single phase without any considerable detectable impurity. Narrow sharp peaks indicate good crystalline nature of the material. All observed reflections were indexed at room temperature. The indexed powder X-ray diffraction pattern of the as-grown crystal ZKP is shown in **Fig. 5.** Simulated X-ray diffraction using single crystal XRD data closely resembles the experimental pattern with varied intensities which could be due to the preferred orientation of the sample used for diffracto meter measurement.

The structure of mixed crystal is elucidated by single crystal XRD and the *ORTEP* is given in **Fig.6a**. The chemical formula of ZKP, as determined by single crystal XRD is $[C_{16}H_{17}KO_{13}]_2Zn$ and it evidences the presence of zinc in the crystalline matrix. The mixed crystal crystallizes in the monoclinic crystal system with centrosymmetric space group $P2_1/c$ and the crystallographic parameters are listed in **Table 2.** The K^+ ions are surrounded by O atom and the K-O bond distance range (2.684 (5)- 3.343 (12) Å) in ZKP crystal is nearly equal to that of Co(II) & Ni(II) phthalate mixed crystal already reported **[22]** the values (2.730(3) - 3.280(8) Å) and slightly higher than Ni(II) phthalate **[23]** (2.670 (9)-3.110(4) Å) and Co(II) phthalate **[24]** (2.63(9) -3.24(4) Å) complexes. The M_2-O (Zn_2-O) distance range in ZKP mixed crystal (2.061(3) - 2.108(3) Å) is in close proximity with the reported values for Co(II) & Ni(II) phthalate mixed crystal (2.040(2) - 2.090(3) Å), Ni(II) phthalate (2.035(3)-2.072(3) Å) and Co(II) phthalate (2.050(2) -2.102(5) Å) complexes. Intramolecular interactions are clearly shown in **Fig.6b**. Crystal packing direction projections along a- ,b- and c- axes are given in **Fig.7.** Along a-axis it appears like a wave- like infrastructure (**Fig.7a)** and packing projection of b- axis is developed like a network

structure consisting Zn connected with K on both sides (**Fig.7b)**. Crystal packing projection along c-axis is given in **Fig.7c**. The polyhedron image of O–H···O intermolecular interactions are clearly displayed in **Fig.8** along with bond distances.

In order to confirm the effect of incorporation of Zn(II) ion on the NLO properties of KHP, the specimen was subjected to SHG test using Kurtz powder method with an input radiation at 4.6 mJ/pulse. The SHG- activity exhibited by some of the centrosymmetric specimens are listed in **Table 3.** The output $I_{2w,}$ a measure of SHG efficiency of ZKP is 112 mV, comparable with that for the reference material, potassium dihydrogen phosphate (122 mV). The second harmonic generation efficiency exhibited by a centrosymmetric specimen could be due to possible local noncentrosymmetry caused by defects or surface effects **[25,26]**. In the present study, the exhibited SHG-activity, contrary to theory, could be justified by the surface defect centers caused by incorporation of foreign metal ion leading to local noncentrosymmetry resulting in nonlinearity at the macro level. We believe that strong and dominant hydrogen bonding interactions are very much responsible for the observed nonlinearity, inspite of a centrosymmetric structure.

4.3.6. Hirshfeld surface analysis

The Hirshfeld surfaces of ZKP have been explained in **Fig.9** by showing *dnorm*, *shape index*, *de* and *di*. The Hirshfeld surface [HF] **[27-29]** surrounding a molecule is defined by points where the contributions of the electron density from the molecules under consideration is equal to the contribution from all the other molecules. For each point on that isosurface, two distances are determined: one is *de* representing the distance from the point to the nearest nucleus external to the surface and second one is *di*, representing the distance to the nearest nucleus internal to the surface. The normalized contact distance *dnorm* **(Fig. 9a**) is based on both *de* and *di*. The surfaces are exposed as transparent to permit visualization of the ZKP, around which they were calculated. The surface representing the spherical impressions (deep red) which are visible on the deep red colour spots in *de* (**Fig. 9c**) are strong interactions such as O···H. The dominant interactions H···O, can be seen in *di* surface plots as the bright red area in **Fig. 9d**. The *shap index* indicates the shape of the electron density around the molecular interactions (**Fig. 9b)**. The small section of area and light colour on the surface represent a weaker or longer interaction other than hydrogen bonds. The two-dimensional fingerprint diagrams **[30]** of ZKP demonstrate the

strong confirmation for the intermolecular interactions. In the fingerprint region (**Fig. 10**), H···O (17.2%) interactions are represented by a spike in the top area whereas O···H (19.3%) interactions are represented in the down part region and both together about 42.4%. The O···K (1.4%) and K···O (1.6%) interactions are represented by a spike in the middle part of fingerprint plot. The H···H interactions (23.5%) are very high in comparison with other bonding interactions. A blunt curved shape at the sides indicates the H···C (7.6%), C···H (10.2%) and bunch like shape represents the O···O (9.1%) interactions.

4.3.7 Micro Hardness Study

Mechanical strength of grown crystal was studied using Shimadzu HMV-2t Vickers microhardness tester with the diamond indenter. By shifting the load of enforced from 25 g to 100 g and the crosswise diameter was determined. Vickers Hardness number Hv was determined using the euation:

$$Hv = 1.8544P / d^2 \ (Kg/mm^2)$$

Where, P is the load and d mean crosswise diameter. The plot between the hardness number with the load is given in Figure 11. It is clearly state that the hardness number is increasing with applied load. The increase in Hv with the increase of load is due to the reverse indentation size effect (RISE)

4.3.8 Z-scan Measurement

Third-order nonlinear optical property of ZKP single crystal was determined using Z-scan technique. The the nonlinear absorption coefficient (β), nonlinear refractive index (n_2) of the missed crystal ZKP was evaluated. In this method, He-Ne laser with beam (632.8 nm) and radius 2 mm was used to analysis the crystal. n_2 was calculated using the following formula,

$$n_2 = \frac{\Delta\varphi}{KI_0L_{eff}}$$

Here $K = 2\pi / \lambda$, I_0 is the intensity of the laser beam at the focus (Z=0), L_{eff} is the effective thickness of our mixed crystal ZKP which was determined by the relation,

$$L_{eff} = \frac{1-\exp(-\alpha L)}{\alpha}$$

Where α- linear absorption coefficient and L - thickness of sample. Closed aperture of Z scan plot was given in Fig.12. In a closed plot, valley followed by peak reveals the positive nonlinear refractive index (n_2) of

material. This suggests that crystal having self-focusing nature. The open aperture Z-scan data, β is determined using the relation,

$$\beta = \frac{2\sqrt{2}\Delta T}{I_0 Leff}$$

Here $\Delta T = 1 - T_v$. (T_v – valley value at open aperture Z-scan curve) Fig.-13. gives the open aperture Z-scan plot. In this figure, minimum transmission occurs near the focus point. This is due to the effect of reverse saturable absorption. Real and imaginary parts of $\chi^{(3)}$ are given by the expressions

$$\text{Re}\,\chi^{(3)}\text{esu} = 10^{-4}\ \varepsilon_0 C^2 n_0^2 n_2 / \pi \quad (\text{cm}^2/\text{W}),$$
$$\text{Im}\chi^{(3)}\text{esu} = 10^{-2}\ \varepsilon_0 C^2 n_0^2 \lambda\beta/4\pi^2 \quad (\text{cm}/\text{W}),$$

Where ε_0 - vacuum permittivity, n_0 - linear refractive index of crystal and the velocity of light – C in vacuum. The absolute value of $\chi(3)$ is determined from:

$$\chi^3 = \sqrt{[\text{Re}(\chi^3)]^2 + [\text{Im}(\chi^3)]^2}$$

The nonlinear parameters such as n_2,β and χ 3 is determined and the values are tabulated in Table-4.

4.4. Conclusion

A new NLO-active mixed crystal ZKP, zinc(II) ion incorporated potassium hydrogen phthalate $[C_{16}H_{17}KO_{13}]_2Zn$ was synthesized and grown from an aqueous solution by slow evaporation technique. Structural analysis of the mixed crystal by single crystal XRD analysis confirms the co-existence of K^+ and Zn^{2+} ions in the mixed crystal. The FT-IR studies clearly indicate the lattice stress in the mixed crystal ZKP. SEM images gives varied external morphologies of ZKP. A centrosymmetric crystal exhibiting SHG efficiency could be due to defect centers resulting in local noncentrosymmetry during laser irradiation. The intra and intermolecular interactions are visually evidenced by the Hirshfeld [HF] surface analysis. Finger print plots quantify the interactions present in ZKP. From the micro hardness measurement, it was informed that the hardness increased with the increase of load until saturation occurred. Even though ZKP crystallizes in a centrosymmetric space group, strong hydrogen bonding interactions facilitate charge transfer leading to nonlinearity. n_2, β, and χ 3 are calculated using Z-scan analysis.

Supporting Information

CCDC 1036083 contains the supplementary crystallographic data for this paper. These data can be obtained free of charge from The Cambridge Crystallographic Data Centre viawww.ccdc.cam.ac.uk/data request/cif.

References

1. D. Xu, D. Xue, Chemical bond analysis of the crystal growth of KDP and ADP, *J. Cryst. Growth,* **2006,** *286*, 108-116.
2. Yan, X.; Xu, D.; Xue, D. SO_4^{2-} ions direct the one-dimensional growth of $5Mg(OH)_2 \cdot MgSO_4 \cdot 2H_2O$, *Acta Mater.,* **2007,** *55*, 5747-5757.
3. Jones, J. L.; Paschen, K. W.; Nicholson, J. B. Performance of Curved Crystals in the Range 3 to 12 A, *J. Appl. Opt.,* **1963,** *2*, 955-961.
4. Yoda, O.; Miyashita, A.; Murakami, K.; Aoki, S.; Yamaguchi, N. Time-resolved x-ray absorption spectroscopy apparatus using laser plasma as an x-ray source**,** *Proc. SPIE Int. Soc. Opt. Eng.*, **1991,** *1503*, 463.
5. Miniwicz, A.; Bartkiewicz, S. On the electro-optic properties of single crystals of sodium, potassium and rubidium acid phthalates, *Adv. Mater. Opt. Electron.*, 1993, *2*, 157-163.
6. Kejalakshmi, K.; Srinivasan, K. Growth, optical and electro-optical characterisations of potassium hydrogen phthalate crystals doped with Fe^{3+} and Cr^{3+}ions, *Opt. Mater.*, **2004,** *27*, 389-394.
7. Shankar, M. V.; Varma, K. B. R. Piezoelectric resonance in KAP single crystals, *Ferroelectr. Lett.*, **1996,** *21*, 55-59.
8. Ashok Kumar, R.; Sivakumar, N.; Ezhil Vizhi, R.; Rajan Babu, D. The effect of Fe^{3+} doping in Potassium Hydrogen Phthalate single crystals on structural and optical properties. *Physica B,* **2011,** *406*, 985-991.
9. Okaya, Y. The crystal structure of potassium acid phthalate, $KC_6H_4COOH.COO$, *Acta Cyrstallogr.*, **1965,***19*, 879-882.
10. Loganayaki, M.; Siva Shankar, V.; Ramesh, P.; Ponnuswamy, M. N.; Murugakoothan, P. Growth and Characterization of Guanidinium Trifluoroacetate – Second Harmonic Generation from a Centrosymmetric Crystal, *J. Minerals & Materials Characterization & Eng.*, **2011,** *10*, 843-853.
11. Shakir, S. K. M.; Kushwaha, K. K.; Maurya, M.; Arora, M.; Bhagavannarayana, G. Growth and characterization of glycine picrate—Remarkable second-harmonic generation in centrosymmetric crystal, *J. Cryst. Growth,* **2009**, *311*, 3871-3876.
12. Nithya, K.; Karthikeyan, B.; Ramasamy**,** G.; Muthu, K.; Meenakshisundaram, S. P. Growth and characterization of Fe^{3+}-doped bis(thiourea)zinc(II) chloride crystals, *Spectrochimica Acta Part A,* **2011,** *79*, 1648-1653.

13. Muthu, K.; Meenakshisundaram, S. P. Growth and characterization of Hexakis(thiourea)nickel(II) nitrate crystals, *J. Cryst. Growth.*, **2012,** *352*,158-164.

14. Chen, H. Y.; Fang, Q.; Lei, H.; Yu, W. T.; Cheng, X. F.; Liu, Z. Q. Structures and nonlinear optical properties of molecular crystals DMCC and DBCC, *J. Mol. Struct.*, **2007,** *871*, 1–5.

15. Ramasamy, G.; Meenakshisundaram, S. Synthesis and crystal structure of potassium hydrogen phthalate mixed crystal $K_{0.78}Na_{1.22}[C_6H_4(COO)_2]\cdot H_2O$, *J. Cryst. Growth*, **2013,** *375*, 26-31**.**

16. Sheldrick, G. M. SHELXL-97, Program for Crystal Structure Solution and Refinement, Release 97-2. University of, Gottingen, Gottingen Germany. **1997.**

17. Kurtz, S. K.; Perry.T. T. A Powder Technique for the Evaluation of Nonlinear Optical Materials, *J. Appl. Phys.* **1968,***39*, 3798-3813.

18. Frisch, M. J. GAUSSIAN-09, Revision C.01, GAUSSIAN, Inc., Wallingford, CT. **2009.**

19. Schlegel, H. B. Optimization of equilibrium geometries and transition structures *J. Comput. Chem.* **1982**, *3*, 214–218.

20. Dennington, R.; Keith, T.; Millam, J. GaussView, Version 5, *Semichem Inc.*, Shawnee Mission KS. **2009.**

21. Kubelka, P. New Contributions to the Optics of Intensely Light-Scattering Materials. Part I**,** *J. Opt. Soc. Am.*, 1948, *38*, 448.

22. Muthu, K.; Bhagavannarayana, G.; Meenakshisundaram, S. P. Synthesis, growth, structure and characterization of nickel(II)-doped hexaaquacobalt(II) dipotassium tetrahydrogen tetra-*o*-phthalate tetrahydrate crystals, *Solid State Sci.*, **2012**, *14*,1355-1360.

23. Biagini Cingi, M.; Lanfredi, A. M. M.; Tiripicchio, A. Structure of (L-alanyl-L-histidinato)copper(II) 3.5-hydrate, [Cu(C9H12N4O3)].3.5H2O**,** *Acta Crystallogr. Sect. C Cryst. Struct. Commun.*, **1984,** *40*, 56–58**.**

24. Furmanova, N. G.; Eremina, T. A.; Okhrimenko, T. M.; Kuznetsov, V. M. Crystal and molecular structures of potassium cobalt hydrogen phthalate $K_2[Co(H_2O)_6](C_8H_5O_4)_4 \cdot 4H_2O$ and mechanism of Co^{2+} impurity trapping in KAP crystals**,** *Crystallogr. Rep.*, **2000**, *45*, 771–774.

25. Fleck, M.; Petrosyan, A. M. Difficulties in the growth and characterization of non-linear optical materials: A case study of salts of amino acids, *J. Cryst. Growth*, **2010**, *312*, 2284-2290.

26. Petrosyan, A. M. Second harmonic generation in centrosymmetric crystal. Comment on the paper by K. Udaya Lakshmi et al., J. Cryst. Growth, *J. Cryst. Growth*, **2009,** *311*, 4538-4542.

27. Spackman, M. A.; Jayatilaka, D. Hirshfeld surface analysis, *Cryst. Eng. Comm.*, **2009,***11*, 19-32.

28. Hirshfeld, H. L. Bonded-atom fragments for describing molecular charge densities, *Theor. Chim. Acta*,1977, *44*, 129–138.

29. Wolff, S. K.; Grimwood, D. J.; McKinnon, J. J.; Turner, M. J.; Jayatilaka, D.; Spackman, M. A. *Crystal Explorer* Version 3.1, University of Western Australia. **2012.**

30. Spackman, M. A.; McKinnon, J. J. Fingerprint plots, *Cryst. Eng. Comm*, **2002,** *4*, 378-392.

Figure Captions

Fig.1. Photograph of mixed crystal KZP

Fig.2. FT–IR spectrum of mixed crystal ZKP

Fig.3. SEM micrographs of ZKP

Fig.4. Direct band gap energy of ZKP

Fig.5. Experimental (red) and simulated (blue) powder XRD patterns

Fig.6 (a) ORTEP (b) 3D image of O–H···O intramolecular interactions

Fig. 7. Crystal packing projection along (a) a-axis (b) b-axis and (c) c-axis

Fig. 8. Polyhedron image of O–H···O intermolecular interactions

Fig. 9. Hirshfeld surface analysis of ZKP (a) *dnorm* (b) *curvedness* (c) *de* and (d) *di*

Fig. 10. Fingerprint plots of ZKP

Table1. FT-IR frequencies (cm^{-1}) and vibrational assignments of ZKP

S.No.	KHP[a]	KZP[b]	Assignment of vibrations
1	1090	1080	ν_{as}(O-H-O)
2	1144	1147	ν_{s}(O-H-O)
3	1445	1475	ν_{as}(O-C=O)
4	1565	1566	ν_{s}(O-C-O)
5	1675	1691	ν_{s}(C=O)
6	3470	3456	ν_{s}(O=H)

[a]Ref [8] [b]Ref [Present study]

Table 2. Crystal data and structure refinement of ZKP

Empirical formula	$C_{16}H_{17}KO_{13}Zn_{0.5}$
Formula weight	489.10
Temperature/K	293
Crystal system	monoclinic
Space group	$P2_1/c$
a/Å	10.4151(4)
b/Å	6.8498(3)
c/Å	29.4743(12)
α/°	90
β/°	98.058(1)
γ/°	90
Volume/Å^3	2081.98(15)
Z	4
ρ_{calc} g/cm^3	1.5602
Absorption coefficient (μ/mm^{-1})	0.883
F(000)	1006.2
Crystal size/mm^3	0.35 × 0.3 × 0.3
Index ranges	$-13 \le h \le 13$, $-9 \le k \le 9$, $-39 \le l \le 37$
Reflections collected	28277
Independent reflections	3664 [R_{int} = 0.0297, R_{sigma} = 0.0231]
Goodness-of-fit on F^2	1.061
Final R indexes [I>=2σ (I)]	R_1 = 0.0475, wR_2 = 0.1367
Final R indexes [all data]	R_1 = 0.0546, wR_2 = 0.1495

Table 3. SHG- activities exhibited by some centrosymmetric crystals

Laser beam wave length (λ)	632.8nm
Lens focal length (f)	18.5cm
Optical path distance (Z)	115 cm
Spot-size diameter infront of the aperture (ω_a)	1 cm
Aperture radius (r_a)	2 mm
Incidentin tensity at the focus (Z=0)	3.13MW/Cm^2
Nonlinear refractive index (n_2)	3.156x10^{-12}cm^2/W
Nonlinear absorption coefficient (β)	-6.7x10^{-4}cm/W
The real part of the third-order susceptibility [Re (χ3)]	1.53x10^{-10}esu
Imaginary part of the third-order susceptibility [Im(χ3)]	7.71x10^{-6}esu
Third-order nonlinear optical susceptibility (χ3)	7.86x10^{-4}esu

System	Centrosymmetric Space group	SHG efficiency	Ref.
Zinc incorporated potassium hydrogen phthalate (ZKP)	$P2_1/c$	~ 0.9 times that of KDP	In this work
Guanidinium trifluoroacetate	*Pbcn*	~ 0.9 times that of KDP	10
Glycine picrate	$P2_1/a$	~ 2.5 times that of KDP	11
Fe^{3+}-doped bis(thiourea)zinc(II) chloride	*Pnma*	~ 0.2 times that of KDP	12
Hexakis(thiourea)nickel(II) nitrate	*C2/c*	~ 0.4 times that of KDP	13
Dibenzoylcroconate	$P2_1/n$	~ 0.6 times that of Urea	14
Potassium sodium phthalate monohydrate	$P3\bar{1}c$	~ 2.2 times that of KDP	15

Table-4:Measurement details and the r sults of the Z-scan technique

Fig.1. Photographs of mixed crystal ZKP

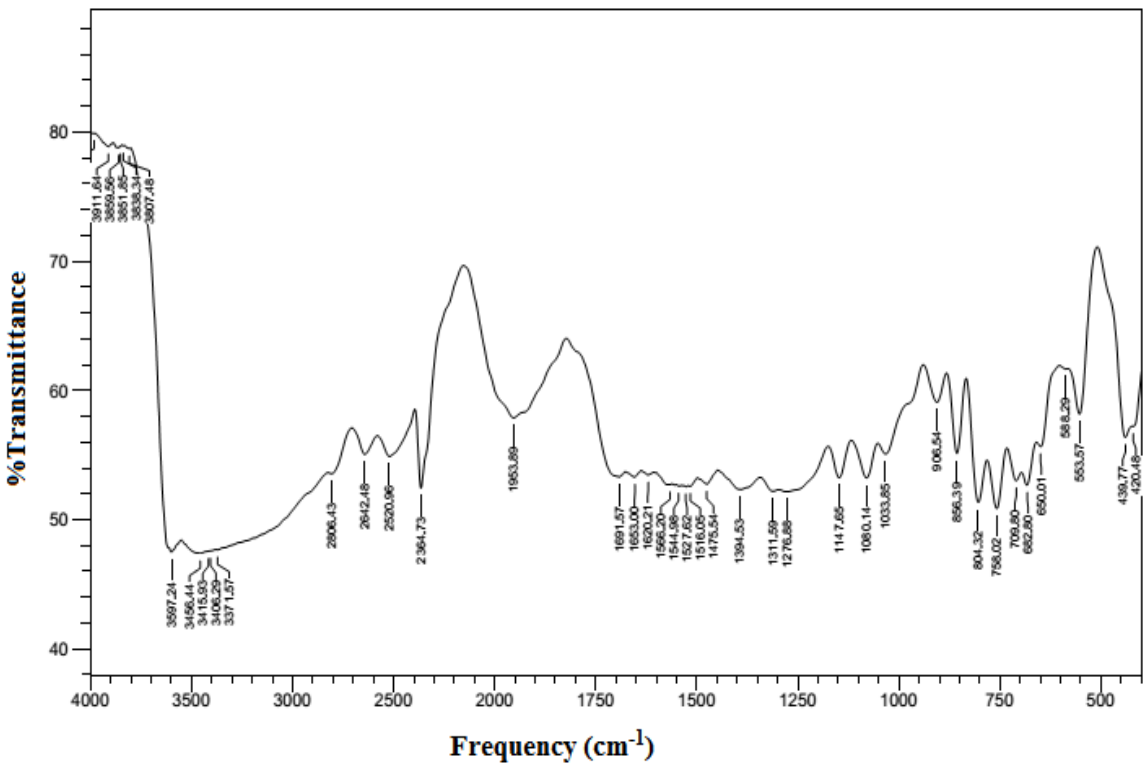

Fig.2. FT–IR spectrum of mixed crystal ZKP

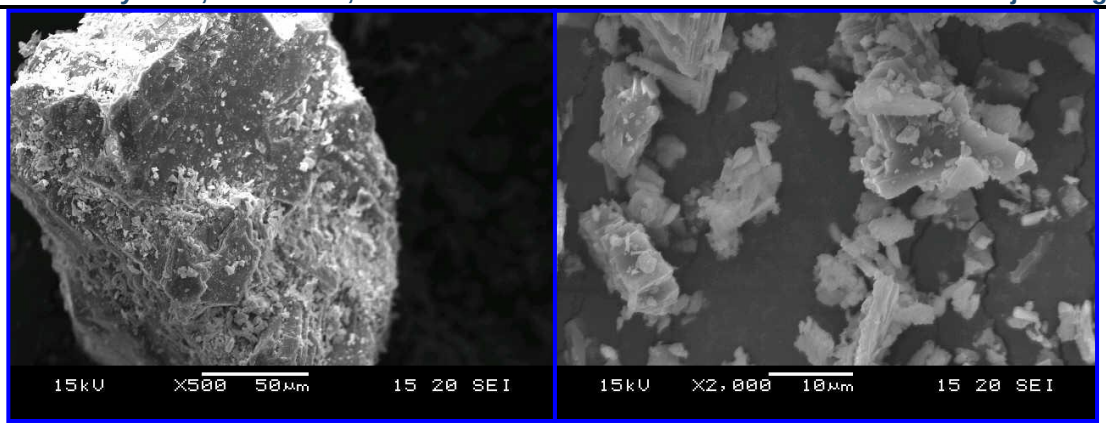

Fig.3. SEM micrographs of ZKP

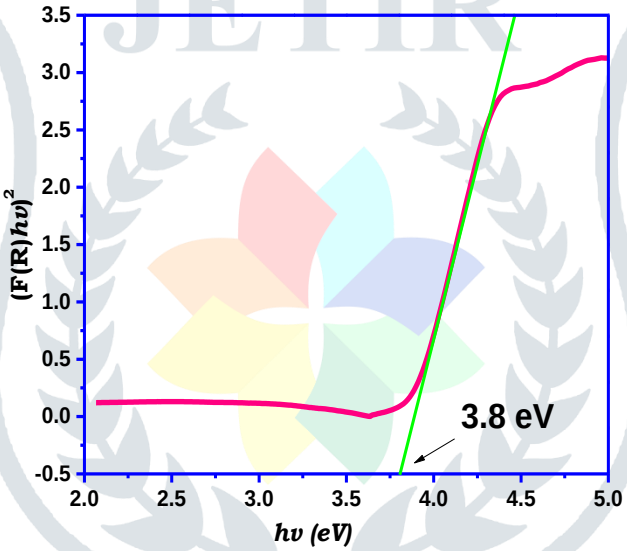

Fig.4. Direct band gap energy of ZKP

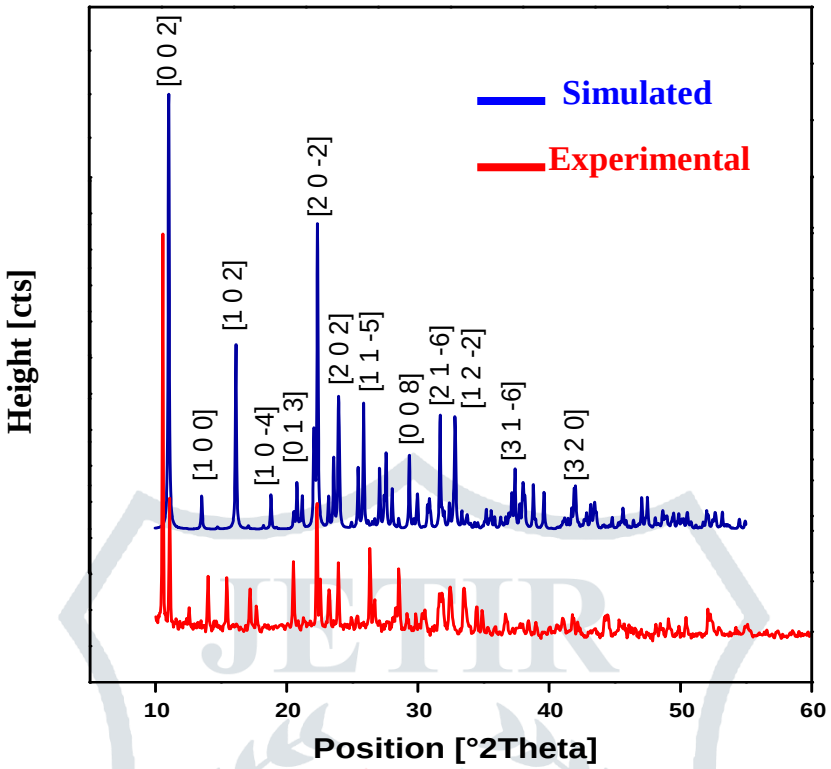

Fig.5. Experimental (red) and simulated (blue) powder XRD patterns

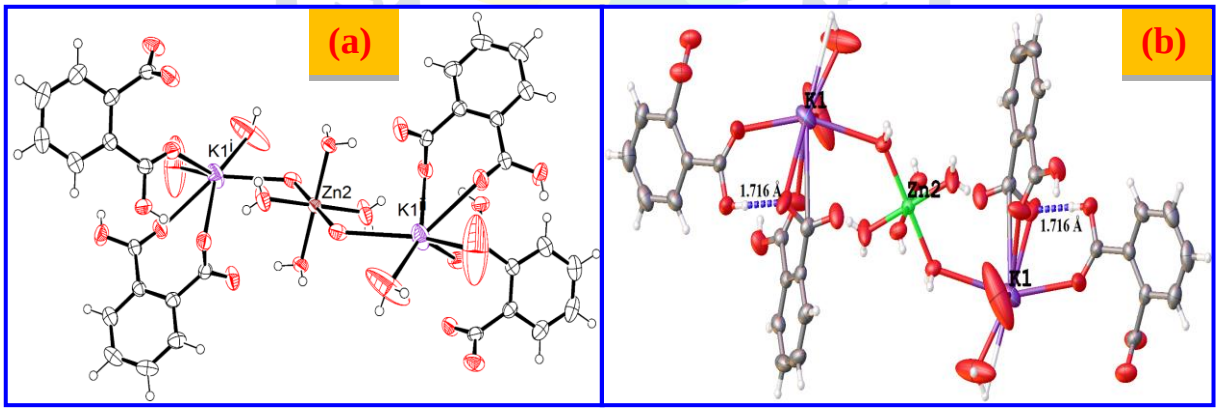

Fig.6 (a*) ORTEP* (b) 3D image of O–H···O intramolecular interactions

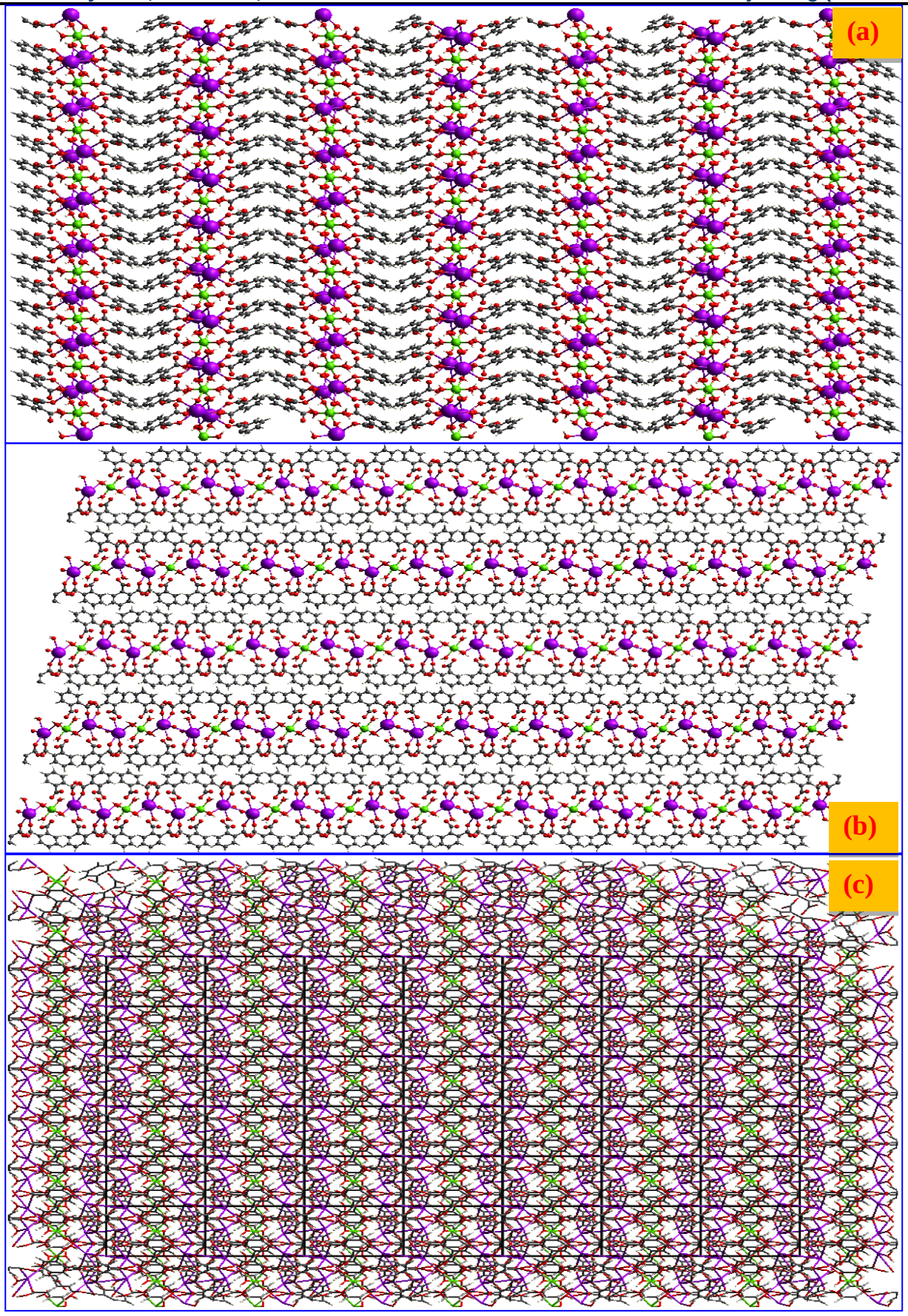

Fig. 7. . Crystal packing projection along (a) a-axis (b) b-axis and (c) c-axis

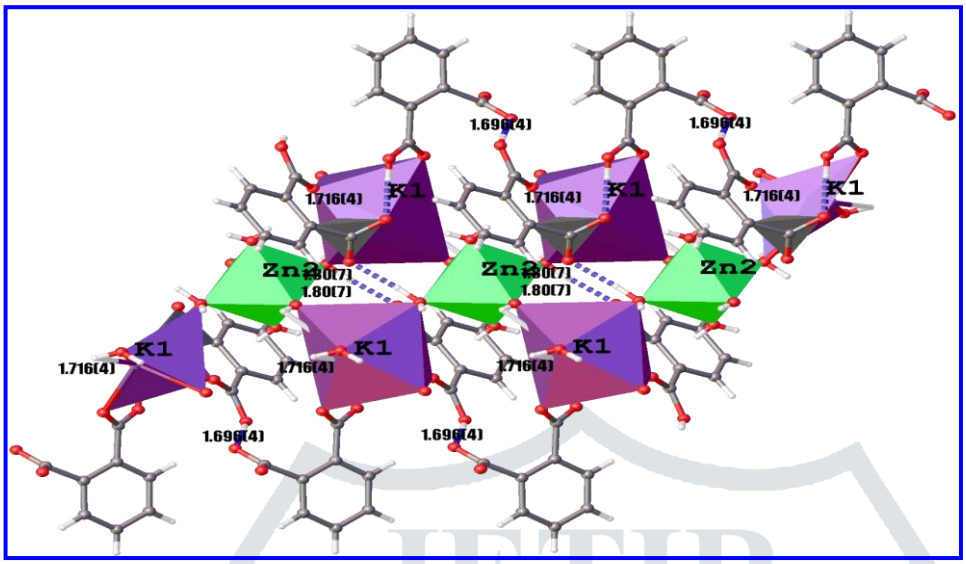

Fig. 8. Polyhedron image of O–H···O intermolecular interactions

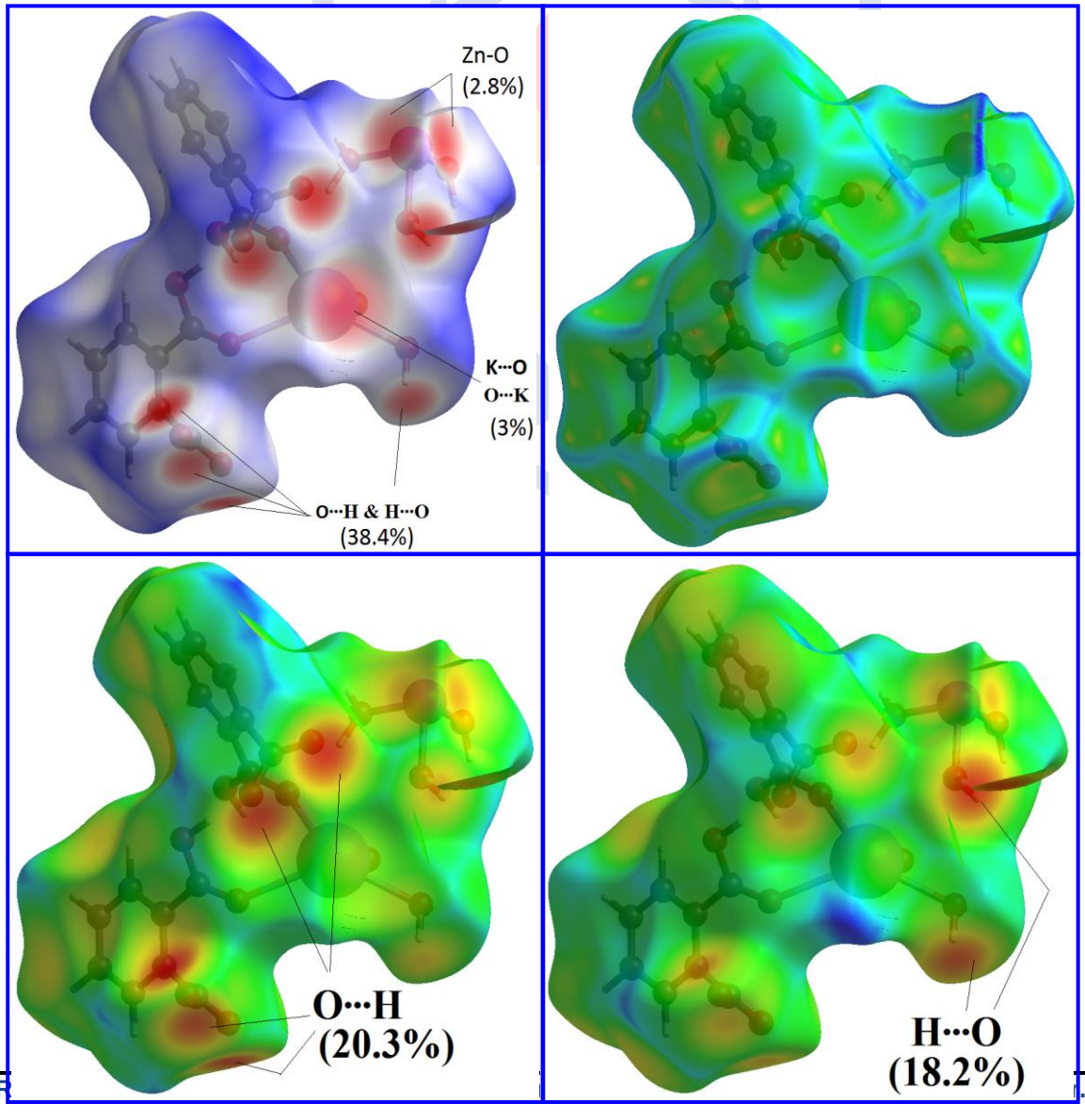

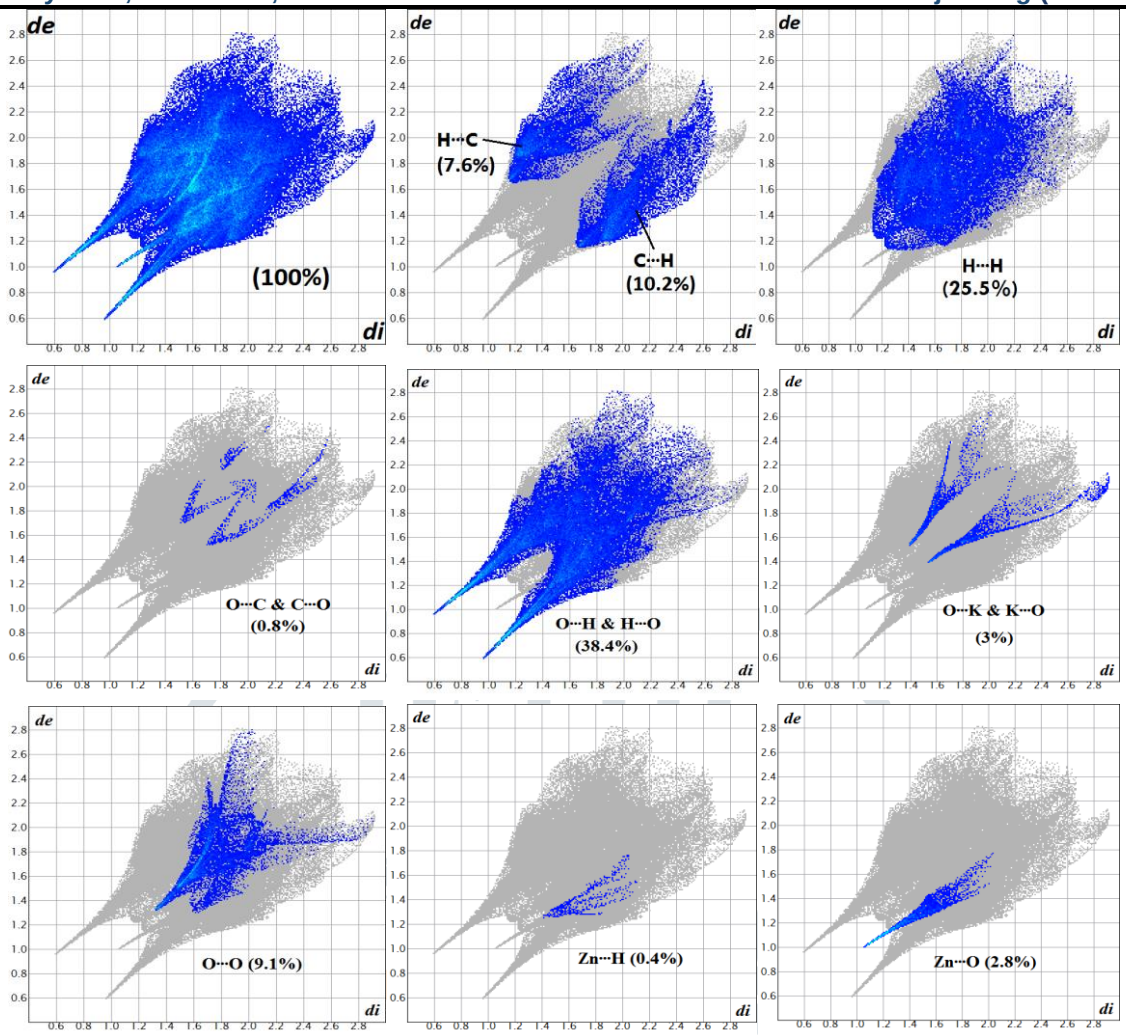

Fig. 10. Fingerprint plots of ZKP

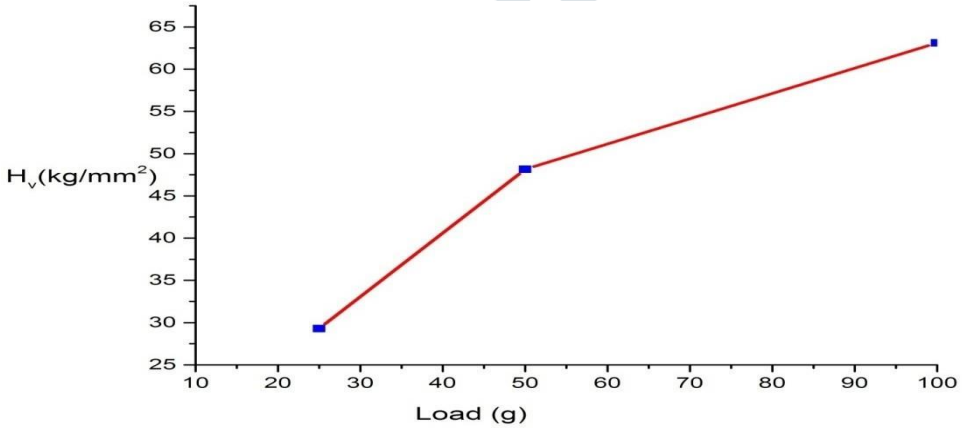

Fig. 11. Variation of H_v for various loads of ZKP

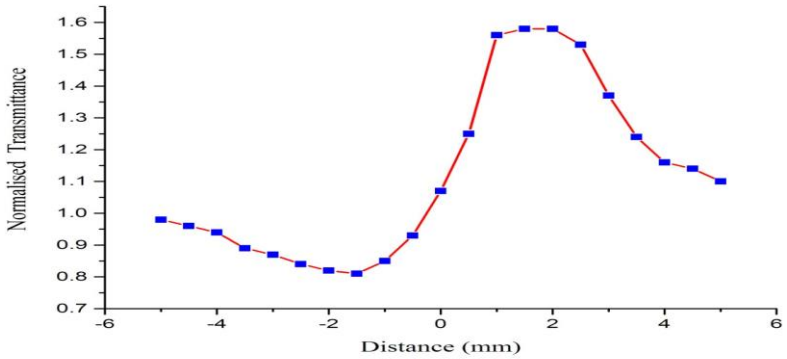

Fig. 12. Closed aperture Z-scan pattern of ZKP crystal

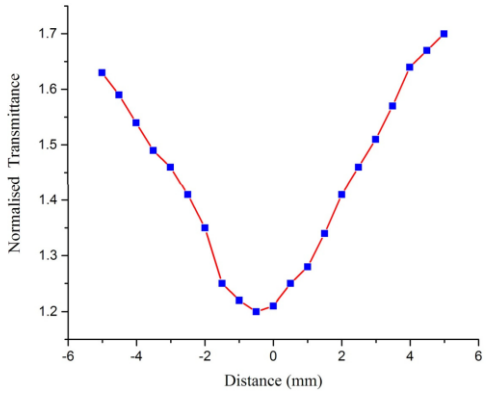

Fig. 12. Open aperture Z-scan pattern of ZKP crystal